Laboratory realization of an ion-ion hybrid Alfvén wave resonator

S. T. Vincena,[1] W. A. Farmer,[1] J. E. Maggs,[1] and G. J. Morales[1]

Received 8 March 2011; revised 20 April 2011; accepted 21 April 2011; published 1 June 2011.

[1] In a magnetized plasma with two ion species, shear Alfvén waves (or guided electromagnetic ion cyclotron waves) have zero parallel group velocity and experience a cut-off near the ion-ion hybrid frequency. Since the ion-ion hybrid frequency is proportional to the magnetic field, it is possible, in principle, for a magnetic well configuration to behave as an Alfvén wave resonator in a two-ion plasma. This study demonstrates such a resonator in a controlled laboratory experiment using a H^+-He^+ mixture. The resonator response is investigated by launching monochromatic waves and sharp tone-bursts from a magnetic loop antenna. The observed frequency spectra are found to agree with predictions of a theoretical model of trapped eigenmodes. **Citation:** Vincena, S. T., W. A. Farmer, J. E. Maggs, and G. J. Morales (2011), Laboratory realization of an ion-ion hybrid Alfvén wave resonator, *Geophys. Res. Lett.*, *38*, L11101, doi:10.1029/2011GL047399.

1. Introduction

[2] A distinguishing feature of shear Alfvén waves in magnetized plasmas with a single ion species is that these waves propagate for frequencies, ω, below the ion cyclotron frequency, Ω, and are evanescent for higher frequencies. The single species cyclotron frequency separating these regimes introduces a particle resonance at which wave absorption occurs, i.e., in the cold plasma limit the perpendicular dielectric coefficient $\varepsilon_\perp \to \infty$, as $\omega \to \Omega$. It has long been established [*Buchsbaum*, 1960; *Smith and Brice*, 1964] that the presence of a second ion species qualitatively modifies the perpendicular dielectric coefficient, which becomes

$$\varepsilon_\perp = 1 - \frac{\omega_{p1}^2}{\omega^2 - \Omega_1^2} - \frac{\omega_{p2}^2}{\omega^2 - \Omega_2^2}. \tag{1}$$

[3] In addition to acquiring another resonant frequency, $\varepsilon_\perp$ can vanish at a frequency commonly referred to as the ion-ion hybrid frequency

$$\omega_{ii} = \sqrt{\frac{\omega_{p1}^2\Omega_2^2 + \omega_{p2}^2\Omega_1^2}{\omega_{p1}^2 + \omega_{p2}^2}}, \tag{2}$$

where ω_{pj} and Ω_j refer to the ion plasma frequency and ion cyclotron frequency of species j, respectively. While the vanishing of $\varepsilon_\perp$ causes a collective resonance for wave propagation across the ambient magnetic field, for shear Alfvén waves (or guided electromagnetic ion cyclotron waves) it results in a wave cut-off for parallel propagation, where wave reflection takes place. This property can be readily seen from the approximate, but highly accurate, dispersion relation for shear waves with large perpendicular wave number $k_\perp$

$$k_\parallel = k_0\sqrt{\varepsilon_\perp}\left[1 - k_\perp^2/k_0^2\varepsilon_\parallel\right]^{1/2}, \tag{3}$$

derived, for example, by *Mithaiwala et al.* [2007]. Here $k_\parallel$ is the parallel wave number, $k_0 = \omega/c$ with c the speed of light, and $\varepsilon_\parallel$ is the dielectric coefficient parallel to the ambient magnetic field. In this context large $k_\perp$ implies that the transverse scale-length is shorter than the smallest ion skin-depth, c/ω_{pj}, in the system. This parameter regime is of significant interest because it allows the modes to interact strongly with both, electrons [*Kletzing*, 1994; *Thompson and Lysak*, 1996; *Chaston et al.*, 2002; *Wygant et al.*, 2002] and ions [*Cornwall and Shultz*, 1971; *Rauch and Roux*, 1982; *Mauk*, 1982; *Horne and Thorne*, 1997]. An additional consequence of this parameter regime is that the compressional mode is evanescent, so that there is no direct coupling or crossover between the shear Alfvén wave and the fast mode for frequencies below the largest Ω_j in the system.

[4] The important role played by the wave cut-off at $\omega = \omega_{ii}$ in determining the structure of low frequency wave spectra has long been recognized in space plasma studies. For instance, *Temerin and Lysak* [1984] identified that the narrow-banded ELF waves seen in the S3-3 satellite were generated by the auroral electron beam in a limited spatial region determined by the local value of ω_{ii} for a mix of H^+-He^+ ions. Recently, the reflection properties for various species concentration scenarios have been investigated [*Hu et al.*, 2010] using a two-dimensional hybrid simulation in a dipole magnetic field. In other theoretical studies it has been recognized that the wave reflection can result in a detached ion-ion hybrid resonator in the equatorial region of planetary magnetospheres. *Guglielmi et al.* [2000] have calculated the resonator spectrum for a parabolic magnetic field and compared it to observations on the ISEE-1 satellite. Their conclusion was that the resonator concept is "plausible, but we have not yet confirmed it experimentally". Further insight into the ion-ion hybrid resonator has been provided by the extensive theoretical study by *Mithaiwala et al.* [2007]. This work concluded that ULF waves excited by the controlled release of gas in the Earth's magnetosphere could be trapped in the resonator formed by typical abundances of H^+-He^+ in the inner radiation belts. In addition to playing a key role in magnetospheric resonators, EMIC waves and the existence of multiple ion species are also important in the scattering of high energy electrons in the inner magnetosphere [*Meredith et al.*, 2003].

[1]Department of Physics and Astronomy, University of California, Los Angeles, California, USA.

0094-8276/11/2011GL047399

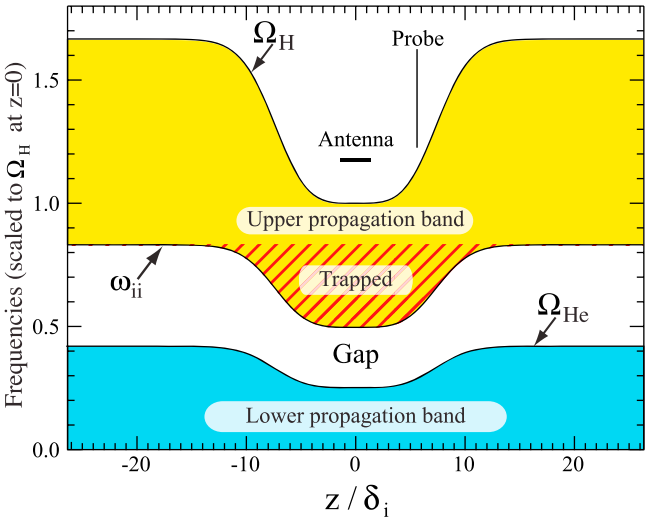

Figure 1. Schematic of axial dependence of experimental magnetic configuration that creates a resonator in an H^+-He^+ plasma with a hydrogen concentration $\eta_H = 0.5$. The bounding black curves indicate the value of relevant frequencies scaled to the H^+ gyrofrequency at the center of the well. Higher frequency shear Alfvén waves, within the yellow band, and lower frequency waves, within the blue band, propagate freely without reflection. Signals at frequencies within the white band labeled 'Gap' are evanescent everywhere. Frequencies within the red crosshatched region are confined to the interior of the well and are candidates for trapped eigenmodes. Axial distance z is scaled to the H^+ inertial length δ_i, calculated at the electron density. The actual axial extent of the antenna is indicated as well as the location of the B-dot probe used to collect the data of Figures 3 and 4.

[5] Motivated by the current interest in this topic the present study reports the first realization of an ion-ion hybrid Alfvén wave resonator in a controlled laboratory environment.

2. Experimental Set-up

[6] The experiments are conducted in the upgraded Large Plasma Device [*Gekelman et al.*, 1991] (LAPD-U) at the Basic Plasma Science Facility at the University of California, Los Angeles. This is a cylindrical device with an overall length of 2070 cm and a main chamber diameter of 100 cm. The plasma is produced using an electrical discharge between a heated, oxide-coated nickel cathode and a molybdenum mesh anode on one end of the device, while an electrically floating copper mesh terminates the plasma at the far end. The main plasma column, between the conducting mesh boundaries is 1660 cm in length (more than 5 wavelengths of typical Alfvén waves) and carries no net current. The typical column diameter is 60 cm, which is more than 300 ion Larmor radii, but does not support propagating, compressional Alfvén waves for the frequencies used in these experiments. Highly reproducible plasma discharges 15 ms long (more than a thousand Alfvén transit times) are repeated at 1 Hz; this allows for the collection of large ensemble datasets using probes with computer-controlled drives.

[7] The plasma densities are typically (1–3) × 10^{12} cm^{-3}, as measured using a swept Langmuir probe calibrated with a microwave interferometer. This yields a typical ratio Ω_e/ω_{pe} ~ 0.3, where Ω_e and ω_{pe} are the electron gyrofrequency and plasma frequency, respectively. Electron temperatures are 5–8 eV during the main plasma discharge, while ion temperatures are approximately 1 eV. This results in a low-beta plasma with $\beta \sim 2 \times 10^{-4}$. The relevant length scale for the Alfvén wave across the background magnetic field is the electron inertial length $\delta_e = c/\omega_{pe}$ while the parallel wavelength scales as the ion inertial length $\delta_i = c/\omega_{pi}$. In the present experiment, $n_e = 1 \times 10^{12}$ cm^{-3}, $\delta_e = 0.53$ cm and for a pure H^+ plasma, $\delta_i = 23$ cm.

[8] The confining axial magnetic field is produced with a set of solenoidal electromagnets controlled by 10 separate power supplies. The device is typically run with a uniform magnetic field strength of 300 G to 2000 G, but the independent supplies allow for a variety of field configurations. Since the ion-ion hybrid frequency is proportional to the strength of the magnetic field, for this study, a magnetic well configuration is formed near the center of the device to establish a resonator, as is sketched in Figure 1. The axial dependence of the confinement magnetic field consists of a low-field uniform segment that is ramped-up on two sides to another region of larger uniform field. The ion-ion hybrid frequency, at which wave reflection occurs and gives rise to axial wave trapping, is encountered in the ramp portions of the well where the field strength increases.

[9] Stable and highly reproducible plasmas can be obtained that consist of two ion species with a concentration ratio that can be continuously selected. Various gas mixtures are produced using fixed-flow settings in independent mass flow controllers that regulate the partial pressures of the individual gases: hydrogen, helium, neon, and argon. Generally, the partial pressures of the neutral gases do not reflect the relative concentration of the ion densities. However, a practical method has been developed [*Vincena et al.*, 2010] that yields reasonably accurate estimates for the ion species concentration.

[10] Shear Alfven waves are excited by inducing field-aligned currents in the plasma. This is accomplished, in this experiment, by using a U-shaped antenna (with right-angle joints) consisting of a bare copper rod (0.48 cm = 0.9 δ_e in radius) with a central section (or bottom of the U) 64 cm in length, aligned with the background magnetic field and positioned at the radial center of the plasma column. The axial extent of this driver is at the mid-point of the column length as shown, schematically, in Figure 1. The two end sections of the antenna (or 'legs' of the U) extend radially outside of the chamber wall, via vacuum feedthroughs. The current path is closed outside of the chamber by connecting the two ends of the U with a wire. The current in the antenna circuit is driven with an RF amplifier with the aid of a 1:1 isolation transformer, so that the entire antenna structure is electrically floating with respect to the plasma and the device. A programmable function generator drives the amplifier input. Monochromatic signals or pulses can be applied.

[11] Wave magnetic fields are measured using magnetic induction probes (i.e., B-dot loops). These probes are constructed of pairs of oppositely-wound induction coils with

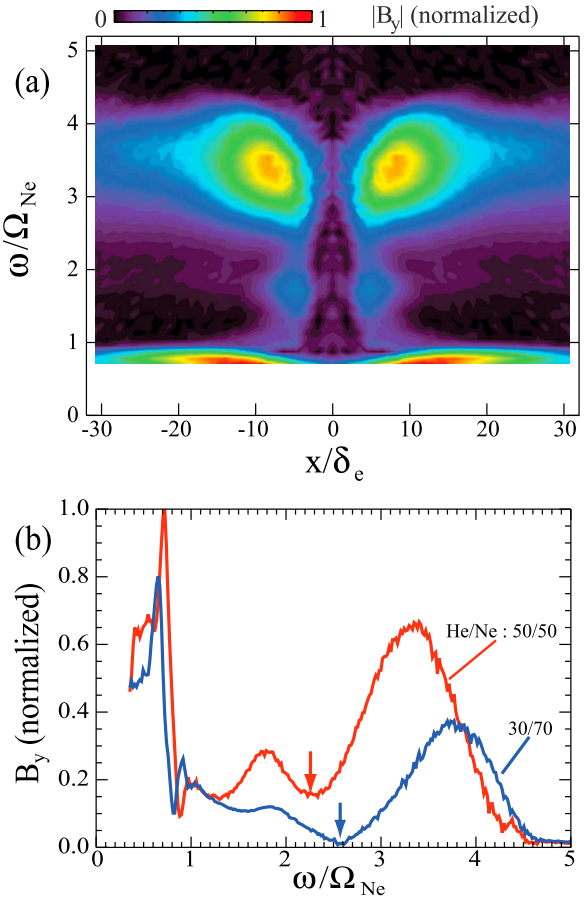

Figure 2. (a) Color contour of the measured amplitude of the wave magnetic field as a function of frequency and position across the uniform confinement magnetic field in a He^+-Ne^+ plasma (n_{He}/n_{Ne} = 1.) Data are acquired for positive *x* values and reflected to negative *x* to show the pattern for an ideal, azimuthally symmetric source. Two propagation bands are separated by a frequency gap. (b) Frequency dependence of wave magnetic field, B_y, at a fixed probe position for two ion concentration ratios: (red) n_{He}/n_{Ne} = 1 (50/50) and (blue) n_{He}/n_{Ne} = 0.43 (30/70). The corresponding ion-ion hybrid frequencies are indicated by the arrows. An ion-Bernstein mode feature is present just below $\omega = 2\ \Omega_{Ne}$.

0.3 cm diameter loops of 50 turns each. A probe comprises 3 such coil pairs with each orthogonal pair measuring the time varying magnetic field along a Cartesian direction. The time series data for each probe is digitized at 12.5 MHz and recorded with 14-bit resolution. Using the phase-locked experimental setup, the time series from between 2 and 8 plasma discharges are averaged together before storage to improve the signal-to-noise ratio. After storage, each probe can be automatically moved (using computer-controlled stepper motors) to a new spatial location, or the wave frequency can be changed as desired, and the process repeated. The recorded voltages are proportional to dB/dt, and signals are numerically integrated to produce B(t).

3. Experimental Results

[12] The properties of shear Alfvén waves in a two-ion plasma, in a uniform magnetic field, were measured in detail and compared to theoretical predictions in a recent publication [*Vincena et al.*, 2010]. To better appreciate the resonator behavior reported here, relevant results from that earlier study are displayed in Figure 2. Figure 2 documents the existence of a wave propagation gap between the lower ion cyclotron frequency and the ion-ion hybrid frequency for a He^+-Ne^+ plasma. The situation in Figure 2a corresponds to detection of the wave magnetic field at an axial position about one wavelength away from the antenna for a uniform magnetic field of 750 G. A horizontal scan is taken across the plasma (the x-direction). For each x position the wave frequency is scanned over the range indicated in Figure 2a. The color contours display the magnitude of the normalized wave magnetic field as a function of x position and frequency (scaled to the Ne^+ gyrofrequency) for a 50/50 He^+-Ne^+ concentration. Red corresponds to the highest wave magnetic field value and black to the lowest. The bright colors near the top correspond to waves propagating between ω_{ii} and the gyrofrequency of He^+ while those near the bottom are due to waves propagating below the Ne^+ gyrofrequency. The smaller amplitude peak (near x = 0) that appears below ω_{ii}, is associated with an ion Bernstein wave, and is discussed in detail by *Vincena et al.* [2010].

[13] Figure 2b illustrates the measured frequency dependence (displayed as the ratio to the neon gyrofrequency Ω_{Ne}) of the wave magnetic field at a fixed x-position for two He^+-Ne^+ concentrations (n_{He}/n_{Ne} = 50/50 red and 30/70 blue). The arrows indicate the estimated values of ω_{ii}. Clear evidence is seen for a propagation gap that is delineated by ω_{ii}. It is this gap property that allows the formation of a resonator in the presence of a magnetic well. The trapped waves propagate in the upper band.

[14] Figure 3 displays the measured response of the resonator at a fixed probe position when a current pulse is applied to the antenna located in the center of the magnetic well, as sketched in Figure 1. The background magnetic field strength ranges from 750 G inside the well to 1250 G outside. The plasma is a 50/50 mix of H^+-He^+. The corresponding axial dependence of the relevant frequencies is shown in Figure 1. The bottom red curve in Figure 3a shows the time dependence of the current pulse in the antenna; the pulse width is comparable to one gyro-period of H^+ at the antenna location, τ_H. The top blue curve shows the time dependence of the transverse magnetic field detected by a probe located inside the well, as indicated in Figure 1. It is seen that the field excited by the pulse displays oscillations at several different frequencies and their amplitudes last longer than two Alfvén transit times inside the well (~7 τ_H.), i.e., the wave packets bounce.

[15] A wavelet analysis of the time series is implemented to better visualize the dynamic evolution of the spectrum excited within the well, as shown in Figure 3b. As a reference, the dashed white curve in Figure 3b shows the wavelet evolution of the current pulse. From the wavelet amplitude, it is apparent that the excitation produces several spectral lines whose amplitudes last longer than the exciter. The long-lasting lines have a frequency larger than ω_{ii} at the bottom of the well and smaller than ω_{ii} outside, i.e., they are in the expected band for trapped modes.

[16] To test that the trapped modes are a direct consequence of wave reflection at the ion-ion hybrid frequency, a study is made of the steady-state response of the resonator for different values of the H^+-He^+ concentration ratio. In this

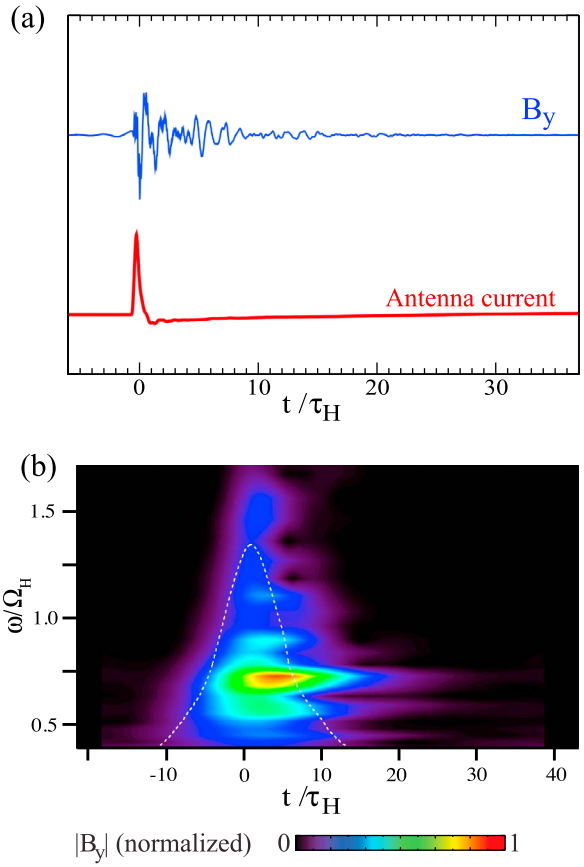

Figure 3. (a) Time dependence of the wave magnetic field B_y (upper blue curve) measured by the probe in Figure 1 in response to an impulse current in the antenna (lower red curve). Time is scaled to τ_H, the H^+ cyclotron period in the center of the resonator. H^+-He^+ plasma with $\eta_H = 0.5$. (b) Color contour of the amplitude of the Morlet wavelet transform of the magnetic field signal in Figure 3a, showing presence of an eigenmode structure. As a reference, the dashed white curve shows the wavelet evolution of the current pulse. Amplitudes before t = 0 are an artifact of the wavelet transform.

case a monochromatic signal is applied to the antenna and the wave magnetic field is measured by a probe at a fixed x position. The frequency is then stepped in discrete intervals over a band from below the He^+ gyrofrequency to above the H^+ gyrofrequency. The frequency scan is then repeated for different values of η_H, the ratio of the density of H^+ to the electron density. The results are displayed in Figures 4a–4c. The green curve (Figure 4a) corresponds to $\eta_H = 0.25$, red (Figure 4b) to $\eta_H = 0.38$, and blue (Figure 4c) to $\eta_H = 0.61$. The semi-transparent horizontal color bars indicate the full extent of the possible eigenfrequencies for each case. Since the waves are launched in the well, propagating frequencies cannot exceed the minimum H^+ gyrofrequency in the well, and trapped waves do not exist above the value of ω_{ii} outside of the well as they are not reflected, but they can propagate away from the source in this band (see Figure 1). Thus, trapped waves should be observed between ω_{ii} inside the well and the smallest of ω_{ii} outside the well and the minimum H^+ gyrofrequency. Indeed it is seen that the wave

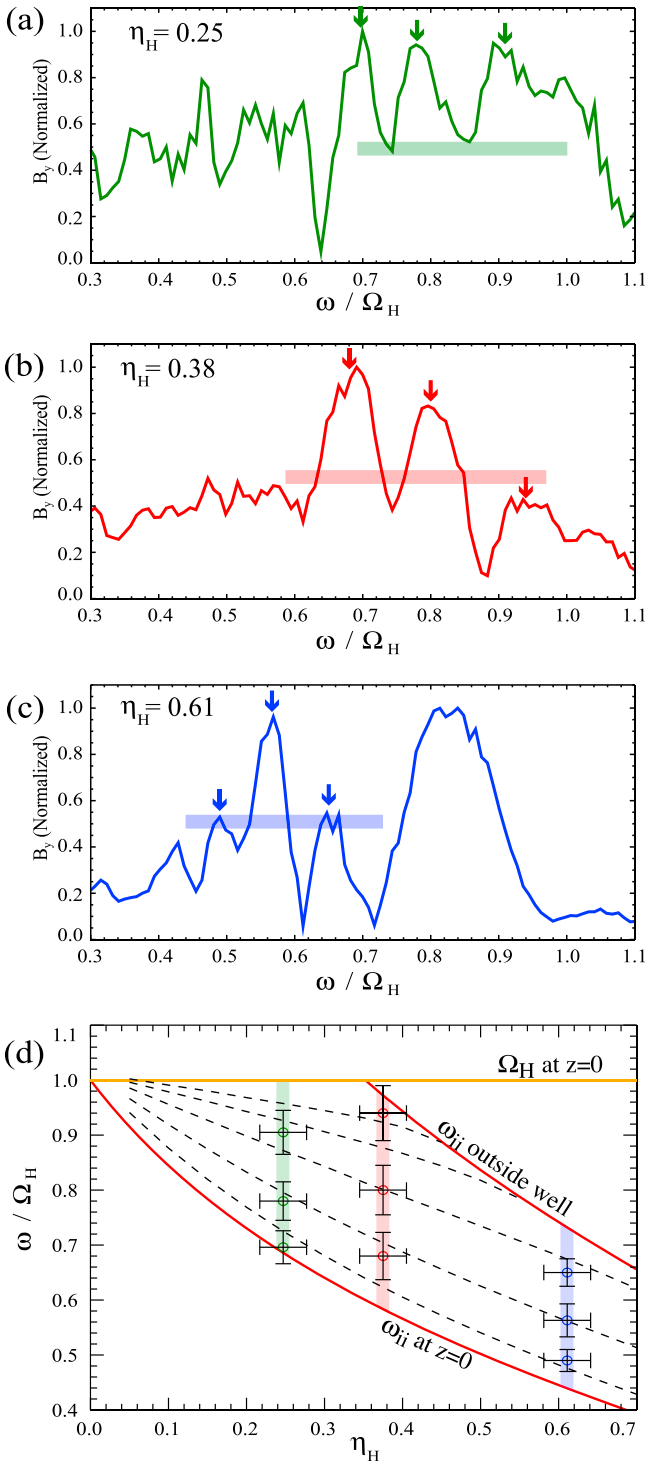

Figure 4. Measured frequency dependence (linear scale) of B_y wave field for different ion concentrations in a H^+-He^+ plasma. Hydrogen concentrations are (a) $\eta_H = 0.25$; (b) $\eta_H = 0.38$; (c) $\eta_H = 0.61$. Arrows mark the locations of prominent observed peaks within the range of possible eigenfrequencies; range is shown as a semi-transparent horizontal band in each panel. (d) Comparison of theoretical (dashed curves) and experimental (colored circles with error bars) resonator frequencies. Vertical color bars correspond to the horizontal bars in Figures 4a–4c.

response shows spectral peaks, limited to the expected trapping band, that change continuously as the concentration ratio is varied. This observation rules out the possible role of wave reflection due to magnetic field gradients because the magnetic configuration is not changed. Wave reflection is due to the presence of two ion species.

[17] An extensive calculation, too lengthy to present here, has been undertaken of the resonator response driven by the antenna for the relevant experimental arrangement; it yields the spatial pattern of the trapped modes and their eigenfrequencies. In Figure 4d the dashed lines represent the predicted values of the eigenfrequencies as a function of the concentration ratio η_H; each dashed curve represents a different axial eigenmode.

[18] The solid red curves in Figure 4d correspond to the maximum and minimum values of ω_{ii} for the magnetic well. The straight horizontal orange line indicates the value of the H^+ gyrofrequency at the bottom of the well. As expected, the predicted resonator eigenfrequencies are bounded by the extremum values of the low-field value of ω_{ii} and the lower of either Ω_H at $z = 0$ or ω_{ii} outside the well, i.e., they are modes trapped between two propagation gaps. The circles (with error bars) represent the observed peaks in the frequency spectrum identified by the arrows in Figures 4a–4c; the circles are color-coded to match curves of the same color. The vertical, semi-transparent bars correspond to the horizontal bars of the same color in Figures 4a–4c. It is seen that the measurements fall within the predicted values. The calculation shows that, for the chosen depth of the magnetic well, the minimum number of axially trapped modes is three, in agreement with the measurement for $\eta_H = 0.61$. However, for lower concentrations of H^+ the close spacing of the higher frequency eigenmodes makes it difficult to resolve the total number of modes.

4. Summary

[19] A controlled laboratory experiment has demonstrated that, in a plasma with two ion species, a magnetic well can create a resonator configuration for shear Alfvén waves (guided electromagnetic ion cyclotron modes). The wave trapping is found to be regulated by the ion-ion hybrid frequency and the measured resonator eigenfrequencies are consistent with theoretical predictions. However, the observed quality factor, Q, of the resonator is on the order of ten or less, indicating that significant wave loss occurs. The detailed mechanism for energy loss merits future, detailed investigation. These laboratory results provide confidence and guidance for the future application of the concept of an ion-ion hybrid resonator to space plasmas.

[20] **Acknowledgments.** This study was sponsored by ONR under the MURI grant N000140710789. The experiments were performed at the Basic Plasma Science Facility (BaPSF) which is jointly supported by DOE-NSF.

[21] The Editor thanks Viacheslav Pilipenko and Craig Kletzing for their assistance in evaluating this paper.

References

Buchsbaum, S. J. (1960), Resonance in a plasma with two ion species, *Phys. Fluids*, *3*, 418, doi:10.1063/1.1706052.

Chaston, C. C., J. W. Bonnell, L. M. Peticolas, C. W. Carlson, J. P. McFadden, and R. E. Ergun (2002), Driven Alfvén waves and electron acceleration: A FAST case study, *Geophys. Res. Lett.*, *29*(11), 1535, doi:10.1029/2001GL013842.

Cornwall, J. M., and M. Shultz (1971), Electromagnetic ion cyclotron instabilities in multicomponent magnetospheric plasmas, *J. Geophys. Res.*, *76*, 7791, doi:10.1029/JA076i031p07791.

Gekelman, W., H. Pfister, Z. Lucky, J. Bamber, D. Leneman, and J. E. Maggs (1991), Design, construction, and properties of the large plasma research device—The LAPD at UCLA, *Rev. Sci. Instrum.*, *62*, 2875, doi:10.1063/1.1142175.

Guglielmi, V. A., A. S. Potapov, and C. T. Russell (2000), The ion cyclotron resonator in the magnetosphere, *JETP Lett.*, *72*, 298, doi:10.1134/1.1328441.

Horne, R. B., and R. M. Thorne (1997), Wave heating of He^+ by electromagnetic ion cyclotron waves in the magnetosphere: Heating near the H^+-He^+ bi-ion resonance frequency, *J. Geophys. Res.*, *102*, 11,457, doi:10.1029/97JA00749.

Hu, Y., R. E. Denton, and J. R. Johnson (2010), Two-dimensional hybrid code simulation of electromagnetic ion cyclotron waves of multi-ion plasmas in a dipole magnetic field, *J. Geophys. Res.*, *115*, A09218, doi:10.1029/2009JA015158.

Kletzing, C. A. (1994), Electron acceleration by kinetic Alfvén waves, *J. Geophys. Res.*, *99*, 11,095, doi:10.1029/94JA00345.

Mauk, B. H. (1982), Helium resonance and dispersion effects on geostationary Alfvén/ion cyclotron waves, *J. Geophys. Res.*, *87*, 9107, doi:10.1029/JA087iA11p09107.

Meredith, N. P., R. M. Thorne, R. B. Horne, D. Summers, B. J. Fraser, and R. R. Anderson (2003), Statistical analysis of relativistic electron energies for cyclotron resonance with EMIC waves observed on CRRES, *J. Geophys. Res.*, *108*(A6), 1250, doi:10.1029/2002JA009700.

Mithaiwala, M., L. Rudakov, and G. Ganguli (2007), Generation of a ULF wave resonator in the magnetosphere by release of neutral gas, *J. Geophys. Res.*, *112*, A09218, doi:10.1029/2007JA012445.

Rauch, J. L., and A. Roux (1982), Ray tracing of ULF waves in a multicomponent magnetospheric plasma: Consequences for the generation mechanism of ion cyclotron waves, *J. Geophys. Res.*, *87*, 8191, doi:10.1029/JA087iA10p08191.

Smith, R. L., and N. Brice (1964), Propagation in multicomponent plasma, *J. Geophys. Res.*, *69*, 5029–5040, doi:10.1029/JZ069i023p05029.

Temerin, M., and R. L. Lysak (1984), Electromagnetic ion cyclotron mode (ELF) waves generated by auroral electron precipitation, *J. Geophys. Res.*, *89*, 2849, doi:10.1029/JA089iA05p02849.

Thompson, B. J., and R. L. Lysak (1996), Electron acceleration by inertial Alfvén waves, *J. Geophys. Res.*, *101*, 5359, doi:10.1029/95JA03622.

Vincena, S. T., G. J. Morales, and J. E. Maggs (2010), Effect of two ion species on the propagation of shear Alfvén waves of small transverse scale, *Phys. Plasmas*, *17*, 052106, doi:10.1063/1.3422549.

Wygant, J. R., et al. (2002), Evidence for kinetic Alfvén waves and parallel electron energization at 4–6 R_E altitudes in the plasma sheet boundary layer, *J. Geophys. Res.*, *107*(A8), 1201, doi:10.1029/2001JA900113.

W. A. Farmer, J. E. Maggs, G. J. Morales, and S. T. Vincena, Department of Physics and Astronomy, University of California, 1040 Veteran Ave., Los Angeles, CA 90095, USA. (vincena@physics.ucla.edu)